A Wireless Multifunctional SSVEP-Based Brain Computer Interface Assistive System

Chin-Teng Lin[1*], Ching-Yu Chiu[1], Avinash K Singh[1,2], Jung-Tai King[2], Yu-Kai Wang[1*]

[1]Centre for Artificial Intelligence, CIBCI Lab, Faculty of Engineering and Information Technology, University of Technology Sydney, Australia
[2]Brain Research Center, National Chiao Tung University, Hsinchu, Taiwan

Abstract— **Several kinds of brain-computer interface (BCI) systems have been proposed to compensate for the lack of medical technology for assisting patients who lose the ability to use motor functions to communicate with the outside world. However, most of the proposed systems are limited by their non-portability, impracticality and inconvenience because of the adoption of wired or invasive electroencephalography (EEG) acquisition devices. Another common limitation is the shortage of functions provided because of the difficulty of integrating multiple functions into one BCI system. In this study, we propose a wireless, non-invasive and multifunctional assistive system which integrates steady state visually evoked potential (SSVEP)-based BCI and a robotic arm to assist patients to feed themselves. Patients are able to control the robotic arm via the BCI to serve themselves food. Three other functions: video entertainment, video calling, and active interaction are also integrated. This is achieved by designing a functional menu and integrating multiple subsystems. A refinement decision-making mechanism is incorporated to ensure the accuracy and applicability of the system. Fifteen participants were recruited to validate the usability and performance of the system. The averaged accuracy and information transfer rate (ITR) achieved is 90.91% and 24.94 bit per min respectively. The feedback from the participants demonstrates that this assistive system is able to significantly improve the quality of daily life.**

Keywords—steady state visually evoked potential (SSVEP); wireless BCI; multifunctional assistive system

I. INTRODUCTION

Brain-computer interfaces (BCIs) have become one of the most promising directions for solving the growing healthcare demand to deal with motor function deterioration caused by ageing, accident or disease [1]. By translating human brain activities into command signals, BCIs enable users to control or communicate directly with devices such as cursors [2-4], wheelchairs [5, 6], spellers [8-10], and cellphones [11] using brain waves, regardless of their neuro-muscular disabilities. The key elements for BCIs to fulfill their goals are determination of target brain patterns [12], signal acquisition, signal processing, and applications [13]. Because BCIs can only deal with specific kinds of brain activity, users must perform specific mental strategies to produce detectable and classifiable brain patterns for BCIs [12]. Once the target brain patterns have been produced by users, BCIs can acquire the EEG signals and process the recorded signal to extract features and make judgements about users' intentions. By combining these brain signal translation techniques with controllable devices such as robotic arms, cursors, and spellers, BCIs can be used in all kinds of applications [2-11].

The most commonly applied brain patterns include steady state visually evoked potential (SSVEP), P300 potentials [14], event-related potentials (ERPs) [15] and motor imagery (MI) [16]. Of these, SSVEP has the advantages of high information transfer rate (ITR), good signal-to-noise ratio (SNR), the need for less training, and the ability to allow a large number of classes [2]. It is adopted in this study for these reasons. The signal acquisition methods can be wired or wireless. While wired acquisition devices provide better signal quality, the bulky hardware, essential cables and necessary preparation procedures for injecting conductive gel dramatically limit the applicability of wired BCI systems. It is therefore necessary to adopt wireless devices and mitigate the influence of signal quality through signal processing methods to construct an applicable and convenient BCI system in real life applications [1].

Methods such as power spectral density analysis (PSDA), canonical correlation analysis (CCA), and signal-to-noise ratio (SNR) are frequently adopted for feature extraction [19] in SSVEP signal processing. However, the performance of these methods may be affected by signal quality when wireless EEG acquisition with a small number of channels is adopted. In this study, we therefore include harmonic frequency information and develop voting mechanisms to improve the system's decision-making performance. Current BCI applications are generally limited to low-degree-of-freedom continuous movement control and discrete selection [18] due to the limitations of known BCI techniques. Combined with the difficulty of multiple subsystem integration, which requires consideration of compatibility between devices, allocation of the computational resources of the system, and placement of hardware devices, this means that there are few wireless multifunctional BCI systems that integrate both robotic control functions and media playback services.

Taking a further step in the construction of BCI assistive systems, we propose and develop a wireless multifunctional SSVEP-based BCI assistive system and ensure its applicability through the refinement of functional menu design and decision-making mechanisms. In this study, we will demonstrate the material and methods, describe the assistive system, give the results and discussion, and lastly present our conclusions.

A. Experimental Setup

A high level stimulating monitor (BenQ XL2430T) with refresh rate of 144 Hz was adopted for the visual stimulation presentation. The presentation method follows the method proposed in [23]. Frequencies of 14.4 Hz, 16 Hz, 18 Hz, 20.6 Hz and 24 Hz, respectively corresponding to ten, nine, eight, seven, six frames of one flickering period of the monitor, were adopted. Considered in this process were the available stable frequencies for the adopted monitor, the SSVEP subsystems for amplitude response [21] and the possible peak shift [22], as a result of which frequencies within the same subsystem, with an interval of at least two Hz, and corresponding to integer frame numbers, were adopted.

Fifteen healthy subjects (thirteen males and two females, overall mean age 23 ± 2.3 years) with normal or corrected-to-normal vision were recruited to participate in the SSVEP experiments, and three of them were invited again for online feasibility test. As we focus more on system integration and usability in current stage of this research, we did not control sex and age factors as other research did [27] when selection participants. None of the subjects had a history of neurological or psychological disorders such as migraine or epilepsy. The purpose and procedures of the experiment were explained to the participants, all of whom completed a consent form before the experiment took place. The experiment comprised three sessions, each containing five rounds; with each round corresponding to one of the five target frequencies. During each round, participants stared for ten seconds at a stimulus corresponding to the frequency of the round. The resting duration was one minute between two sessions and ten seconds between two rounds.

O1 and O2 channels of Mindo 4S with spring-loaded dry sensors were adopted for the EEG acquisition in the SSVEP experiment and placed according to the international 10-20 system. The Mindo 4S, sampling at rates of 250 Hz, was designed and developed by the Brain Research Center, National Chiao Tung University [20]. No conductive gel or skin preparation was necessary. All EEG signals were recorded, amplified and band-pass filtered between 0.24 and 125 Hz.

B. Signal Analysis

This section describes the data analysis methods and procedures and details of the following: data segmentation, feature extraction, voting mechanisms, and evaluation methods.

1) Data segmentation

As demonstrated in our previous work [26], the suitable data length for each decision trial is five seconds. Each recorded ten-second trial can be converted into six five-second trials, as shown in Figure 1. Following our previous procedures, the first decision is made at the fifth second using the data from the zeroth second to the fifth second, and the next decision is made in every subsequent second. That is to say, the second decision is made at the sixth second using the data from the first second to the sixth second.

2) Feature extraction

In this study, the power values derived by fast Fourier transform (FFT), the signal-to-noise ratio (SNR) of the power peaks and the correlation values calculated using canonical-correlation analysis (CCA) are adopted as the features for the SSVEP BCI to use to classify each five-second decision trial. To improve performance, the effect of harmonic frequency components is also considered.

For every five-second trial, FFT is applied to two channels separately. The derived power spectrum is used as the first feature. SNR is then applied to the power spectrum to produce the second feature. Taking P_n as the power value of n Hz, formula (1) shows the calculation of the SNR of n Hz for a single channel's data. In each five-second trial, where $n=14.4, 16, 18. 20.6, 24$, if P_n is maximized when $n=16$, the trial is categorized as taking place when the subject is staring at the 16Hz option in the FFT feature. Following the same rule, if the SNR (of n Hz) reaches maximum when $n=18$, this trial will be judged as the signal for the 18Hz option in the SNR feature.

$$\text{SNR (of } n \text{ Hz)} = \frac{P_n}{(P_{n-1}+P_{n-0.5}+P_{n+0.5}+P_{n+1})/4} \quad (1)$$
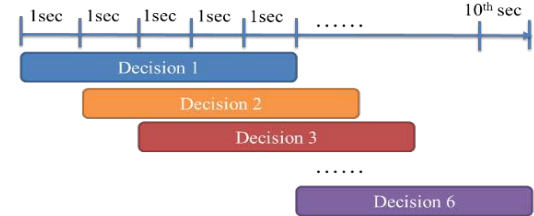

Figure 1. Data segmentation. Decisions are made from the fifth second and one by one in every next second. Data from the zeroth second to the fifth second make the first decision. Data from the first second to the sixth second make the second decision, and so on. Following the same rule, data from the fifth second to the tenth second will make the sixth decision.

Another widely adopted method for SSVEP BCI is CCA, which aims to find a pair of linear transforms for any two given datasets such that the two transformed datasets have maximized correlation [19]. In this study, we use the correlation between the recorded five-second trial and a reference signal with frequency F to judge the degree to which this trial correlates with a flickering of frequency F, where F=14.4, 16, 18, 20.6, 24. If the correlation value is maximized when F=14.4, we judge that this trial is recorded when the user is staring at 14.4 Hz. As will be mentioned later, we also adopt the second harmonics of the five frequencies as F to produce different CCA features, i.e. F=28.8, 32, 36, 41.2, 48.

It has been reported that the harmonic components also help to improve accuracy [24]. Considering that the response amplitude of SSVEP drops significantly as the frequency gets higher, we only take account of the first three orders of harmonics. To reduce the computational cost, we do not use complicated formulas to extract the features of the target harmonic components but simply apply three methods to sum the target power values and compare levels of accuracy to determine the best method. In method 1, we adopt the summations of power values of the first three orders of harmonics as features for five target options, as listed in Table

1. The summation is noted as S_n, $n = 14.4, 16, 18, 20.6, 24$. If the maximum of S_n appears when $n = 14.4$, we judge the trial to be recorded when the subject is staring at the 14.4 Hz option. Considering the existence of the 60Hz AC noise in our environment, the power value $P_{61.8}$ is excluded and the summation of $P_{20.6}$ and $P_{41.2}$ increased 1.5 times to compensate for the missing item. In method 2, we exclude P_{72} because 72 Hz is outside the three SSVEP subsystems and the response amplitude compared to others [21] is theoretically too small. All summations in method 2 are then averaged to compensate for the difference in the number of items. In method 3, we adopt only the first two orders of harmonics to avoid problems of AC noise and amplitude drop of high frequency bands, and this method also makes the number of items of each S_n equal.

TABLE 1. ACCURACY COMPARISON OF THREE HARMONIC ADOPTION METHODS.

Method 1		Method 2		Method 3	
$S_{14.4} = P_{14.4} + P_{28.0} + P_{43.2}$ $S_{16} = P_{16} + P_{32} + P_{48}$ $S_{18} = P_{18} + P_{36} + P_{54}$ $S_{20.6} = (P_{20.6} + P_{41.2}) \times 1.5$ $S_{24} = P_{24} + P_{48} + P_{72}$ * Considering a 60hz noise peak		$S_{14.4} = (P_{14.4} + P_{28.0} + P_{43.2})/3$ $S_{16} = (P_{16} + P_{32} + P_{48})/3$ $S_{18} = (P_{18} + P_{36} - P_{54})/3$ $S_{20.6} = (P_{20.6} + P_{41.2})/2$ $S_{24} = (P_{24} + P_{48})/2$ * Considering 72hz is too weak		$S_{14.4} = P_{14.4} + P_{28.0}$ $S_{16} = P_{16} + P_{32}$ $S_{18} = P_{18} + P_{36}$ $S_{20.6} = P_{20.6} + P_{41.2}$ $S_{24} = P_{24} + P_{48}$ * To equalize # of items.	
O1	O2	O1	O2	O1	O2
38.67%	40.52%	**51.48%**	**52.30%**	45.33%	48.15%

The last two rows in Table 1 show the classification accuracy of the O1 and O2 channels using the three methods. It is clear to see that method 2 outperforms the others in both channels, thus this method is selected for the adoption of harmonic components. Another important result is that accuracy is quite poor when the features of only one channel are used. This has motivated us to develop voting methods to improve the results.

C. Integrated Assistive System

Figure 2A shows the configuration of the system. The complete system can be divided into three parts: the SSVEP BCI system, an assistive eating system, and a video playback system. The SSVEP BCI system is composed of the wireless EEG cap, Mindo 4S, a high refresh rate monitor, and a computer host. The assistive eating system is composed of a meal box as a food container, a robotic arm for food pickup and delivery and a web camera for mouth position detection. The video playback system, which enables users to watch films or news, make video calls, or play a pre-recorded voice message to request help from friends nearby, is comprised of the monitor and the speakers connected to the computer host.

The operation flowchart of the system is shown in Figure 2B. When subjects mentally select an option and stare continuously at a target function on the main menu, the system detects and processes the underlying EEG pattern in real time. This information is subsequently used to trigger the selected service system. Figure 2C shows the block diagram of the integrated multifunctional assistive system. As shown, the SSVEP BCI system transforms the user's EEG signal into commands and

triggers the selected services of the two subsystems, the assistive eating system and the video playback system. A subjective adjustment option is included in this system which contains a series of training procedures for new users to pre-adjust the parameters of the SSVEP BCI system to improve system accuracy and performance. As shown in Figure 2C, there are five options in the main menu when a user starts the system. Four of the options are services: eating assistance, video entertainment, active interaction, and video call. As presented in our previous work [26], the eating assistance service has five options in the service menu consisting of three kinds of food, one option for water, and one exit option. In this study, we extend the same five-option SSVEP BCI to include video playback functions through the multilayer design of the menu. Each of the video playback services also contains five options.

In this study, three subsystems including a wireless SSVEP-based BCI, a robotic assistive eating system, and a video playback system are integrated using C# language. The details of each system will be described in the paragraphs below.
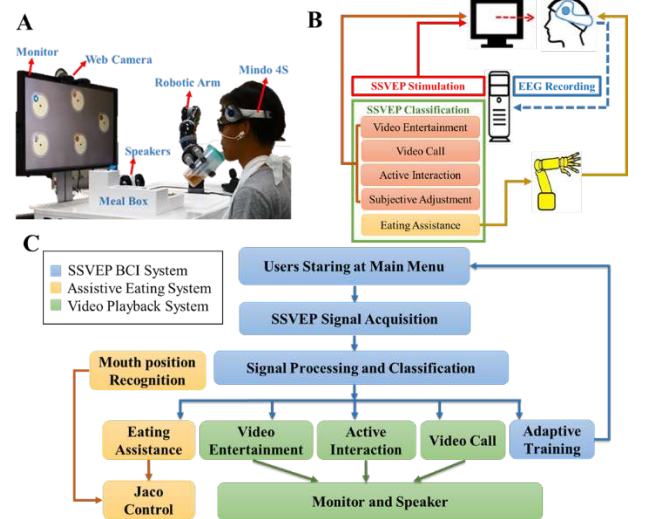

Figure 2. Wireless multifunctional SSVEP-based BCI assistive eating system. (A) System configuration. The components of this system include a computer host, a wireless EEG cap, Mindo 4S, a robotic arm, a set of speakers, a meal box, a high refresh rate monitor and a web camera. The SSVEP BCI function of this system is executed by Mindo, the monitor, computer host. The robotic arm and web camera control the eating assistance service. Video playback services are presented by the speakers and the monitor. (B) Operation flowchart. The computer host sends the SSVEP stimulation command to the monitor and collects the EEG data recorded by Mindo 4S via Bluetooth transmission. It then executes SSVEP classification and sends the command to the corresponding subsystem to complete the task. (C) Block diagram of the integrated assistive eating system. The SSVEP BCI system transforms the user's EEG signal into commands and triggers the selected service of the two subsystems, the assistive eating system and the video playback system. A subjective training option is also included in this system to optimally adjust the model for the current user in a short training period.

1) Wireless SSVEP-based BCI

The wireless SSVEP-based BCI is the core of the assistive system. It records a user's brain signals, processes and translates the signals into commands representing the user's intentions, and transmits the commands to the corresponding subsystems. To enhance system usability and convenience, a wireless and

portable EEG Mindo 4S is adopted. This four-channel EEG cap, Mindo 4S, was developed by the Brain Research Center of National Chiao Tung University in Hsinchu, Taiwan. Equipped with spring-loaded sensors which enable electrodes to contact the scalp through the hair, Mindo 4S can record usable EEG data with good quality after simply putting it on [20]. Table 2 shows the Mindo 4S specifications.

TABLE 2. MINDO 4S SPECIFICATIONS.

Channel	4
Sample rate	512 Hz Max.
Gain	800
Frequency Response	0.24Hz TO 125 Hz
Recording time	Up to 20 hours
Interface	Micro USB 2.0
RF	Bluetooth 2.0
Battery	3.7V Lithium Cell
Weight	~100g

The visual stimuli are designed in the shape of circles in black and white and presented with 100% contrast. The angular size of the stimuli is ~7.86° in average. Figure 3 shows the visual stimuli and menu. Small icons indicating functional options are embedded in upper left of each stimuli as shown in Figure 3B. Flickering frequencies of 14.4Hz, 16Hz, 18Hz, 20.6Hz, 24Hz are coded at a monitor with a 144Hz refresh rate. Details of the experiment procedures and design are given in Section II.
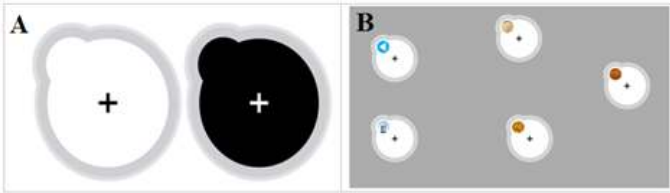

Figure 3 (A) Layout of visual stimuli. (B) Menu layouts.

2) Assistive eating system

The robotic assistive eating system is composed of a robotic arm, a meal box, and a web camera for mouth detection. The Jaco robotic arm (version AM3240 0003) by Kinova Robotics is used. All the moving trajectories required for Jaco to execute the various tasks are pre-recorded using the Jaco application programming interface, with the exception of the position of the user's mouth, which is determined by a mouth detection program. Once the user starts the assistive eating function, the mouth position detection software detects the position of his/her mouth and sends the information to the main program. After a selection has been made by SSVEP-based BCI, the main program adds the position information to the trajectory corresponding to the selected service. Jaco then picks up the selected food/water option, delivers it to the mouth position, and waits for the user to consume it.

3) Video playback and calling system

The services provided by the video playback system have three options: video entertainment, video calls, and active interaction. Each of the three categories contains four options and one exit option. The video entertainment service allows the user to watch online news, preselected music videos or movies. The video call service is performed by commanding the program to call one of the four sets of phone numbers predefined by the user. The web camera function enables the user to exit a film during play by turning his/her head away for five seconds. If the mouth detection system is unable to detect the user's eyes and mouth for five seconds, play will cease. An active interaction service is designed for users who have difficulty speaking. It allows a user's caregiver to prerecord four voice messages to request help; for example, asking to go for a walk, expressing discomfort, asking to go to the toilet, or asking to take a rest. When a user enters the active interaction service, the system plays the voice command corresponding to the user's request to a nearby caregiver.

D. Performance Evaluation

1) Voting mechanisms

Since there is an exit option on every function page, misclassification may lead to unpleasant function page switch and cost users much time to switch back. We therefore extend the four-vote voting mechanism from our previous work [26] to improve classification accuracy and reduce the number of misclassification trials. Below, we describe the structure of the extended voting methods using six and seven votes.

Figure 4 shows the structure of six-vote and seven-vote mechanisms. In Figure 4A, we adopt six different features calculated from O1 and O2 channels, each of which produces one answer/judgement. We then organize the six answers using voting methods and test the different threshold settings to find the best one. The threshold was adopted as the criterion of skipping the trial or not. As mentioned, misclassification in this system will significantly reduce usability. At the same time, brain activity or patterns may not always clearly indicate an option. For reducing the number of misclassified trials, one solution is adopting a threshold to handle the trials in which the features are not clear. Five kinds of threshold are compared, as shown in Figure 4A. First four thresholds requesting the number of answers voting for same options to be greater than specific values including three, four, five or six, otherwise the system would skip the trial without making a final answer. The last criterion will produce the final answer based on the maximum number of votes.
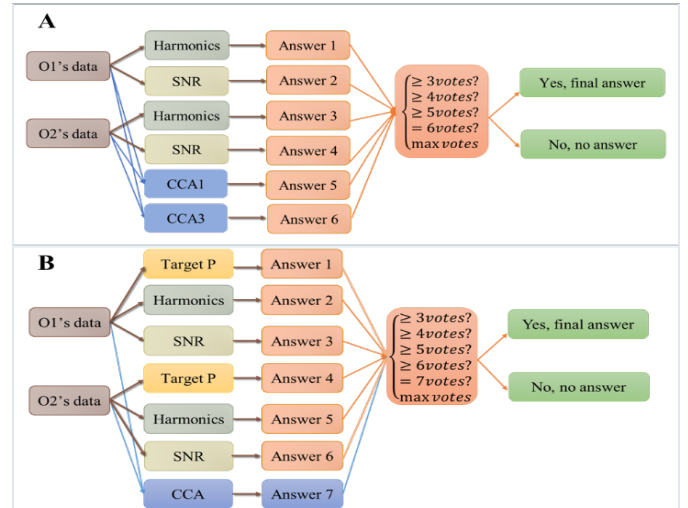

Figure 4. (A) Structure of six-vote mechanism. (B) Structure of seven-vote mechanism.

Figure 4B shows the structure of the seven-vote mechanism. The structure follows the same rules as the six-vote mechanism; the major difference is in the adopted features. The reason for adopting the six-vote and seven-vote mechanisms with the features shown in Figure 4 is that a comparison of all the combinations of different numbers of votes with different features demonstrates that the best performances are achieved by the methods shown in the figure. Figure 4A shows that the power values of the harmonics and SNR for each channel are calculated using the methods previously described. The correlation of both channels' data is also calculated. Note that the calculation of all CCA follows the procedures explained in previous sections, while CCA1, CCA2 and CCA3 adopt different reference signals. As shown in Table 3, CCA1 adopts the signals of five target frequencies as the reference signal, while CCA2 adopts only the second order harmonic of the target frequencies, and CCA3 is the sum of CCA1 and CCA2. Because more channel numbers increase the performance of CCA [25], the data of both channels is always combined as one input for all CCA methods. The comparison results are shown in Section III.

2) Evaluation methods (ITR, acc, execution rate)

To evaluate the performance of each method, information transfer rate (ITR), classification accuracy and execution rate are applied in this study. ITR ($Bits/min$) is a commonly used index for evaluating the performance of a BCI system. The definition of ITR is described in equation (2), where N is the number of targets, P is the accuracy of target identification by the classification system and T is the stimulation duration (seconds) for a selection.

$$\text{ITR} = \left(\frac{T}{60}\right)^{-1} \times \left[\log_2 N + P\log_2 P + (1-P)\log_2 \frac{(1-P)}{(N-1)}\right] \qquad (2)$$

Because there are skipped trials in our system, accuracy is redefined as the ratio of number of correct trials and number of answered trials as shown in (3). To further investigate the performance of our system, the execution rate defined as the ratio of number of correct trials and number of total trials is also calculated (4). Note that the stimulation duration T is influenced by the execution rate as shown in (5). A higher execution rate indicates that the system has skipped fewer trials, therefore the duration of the stimulation will be shorter.

$$ACC = \frac{\# \, of \, Correct \, trials}{\# \, of \, Answered \, trials} \, (\%) \qquad (3)$$

$$Execution \, rate = \frac{\# \, of \, correct \, trials}{\# \, of \, total \, trials}(\%) \qquad (4)$$

$$\text{T} = \frac{total \, stimulation \, time}{\# \, of \, total \, trials} \div \text{execution rate} \qquad (5)$$

III. RESULTS AND DISCUSSION

A. Algorithm performance

Table 3 shows the performance of the original features without voting. Motivated by the improvement made by adopting harmonic components [24], we were interested to investigate whether the CCA results for harmonic components

would also benefit performance. We therefore compare three kinds of CCA features in Table 3. The first feature is the original method as explained in previous sections. We combine the O1 and O2 channel data and applied CCA to derive the correlation values of the combined EEG data and reference signals of five target frequencies. For the second feature, we only calculate the correlation values between the combined EEG data and the reference signals of second order harmonic frequencies. For the third feature, we sum the first two features as the third feature.

Note that because no trials are skipped, the execution rate not shown here would be same as accuracy. As shown in Table 3, the accuracy and ITR performance is quite poor when single features are used for classification. The number of wrong trials may be even higher when only target power or SNR are used as features, which makes this method unsuitable for our proposed system. The ACC and ITR performances are significantly improved when the CCA method is used; however, the averaged ACC is still below 80%, thus the number of wrong trials is still too high for the system to be acceptable. This situation reveals the difficulty that may be encountered when only two channels are used, without conduction gel or channel preparation being applied prior to the experiment. To compensate for the lack of signal quality, voting mechanisms equipped with a decision-making threshold to skip trials with no clear user intention are adopted and compared.

TABLE 3. PERFORMANCE OF ORIGINAL FEATURES.

Feature	ACC	Correct	Wrong	ITR
Target Power (O1)	46.59%	629	721	4.31
Target Power (O2)	52.52%	709	641	7.07
SNR (O1)	45.56%	615	735	3.92
SNR (O2)	51.78%	699	651	6.68
Harmonic (O1)	51.48%	695	655	6.53
Harmonic (O2)	52.30%	706	644	6.95
CCA1 (only targets)	66.96%	904	446	17.98
CCA2 (only harmonics)	58.44%	789	561	10.76
CCA3 (targets + harmonics)	72.30%	976	374	23.85

The results of the four-vote method proposed in previous work [26] are also calculated and shown in Table 4 to make the comparison more complete. From the results, we can see that using SNR and harmonics as features for the four-vote method results in much-improved accuracy of 81%. However, the

number of no answer trials is fairly large, thus the system execution rate is significantly suppressed. Another problem is that the number of wrong trials is still large enough for the system to make frequent mistakes.

TABLE 4. RESULTS OF 4 VOTE MECHANISM.

Feature	ACC	Correct	Wrong	Skipped	Exe Rate	ITR
Target P + SNR	73.23 %	503	183	664	37.26 %	12.76
Target P + Harmonics	74.47 %	531	182	637	39.33 %	14.05
SNR + Harmonics	**82.73 %**	**527**	**110**	**713**	**39.04 %**	14.89

Table 5 shows the performance of the six-vote method. It is clear that accuracy is improved and that the number of wrong trials is also effectively suppressed as the applied method or threshold becomes higher.

Table 6 shows the performance of the seven-vote mechanism. Note that the CCA voter in this table applies the first CCA feature mentioned in Table 3 (CCA1), which does not consider the harmonic components. There is a clear trend that, as more voters are included, accuracy increases, and the number of misclassified trials is suppressed. Table 7 demonstrates the adoption of the best features in Table 3 (CCA3), which includes both target frequency and harmonic information. Compared to the results in Table 6, using both target frequencies and harmonics as CCA features could produce more correct trials and fewer wrong trials. Note that the best ITR of 29.43 is achieved by the six-vote method shown in Table 5, and the second highest ITR of 29.21 is also achieved by the six-vote method. This demonstrates the effect of the execution rate.

TABLE 5. RESULTS OF 6 VOTE MECHANISM.

Method	ACC	Correct	Wrong	Skipped	Exe Rate	ITR
>=3	80.09%	917	228	205	67.93%	29.43
>=4	**89.31%**	**677**	**81**	**592**	**50.15%**	**29.21**
>=5	**95.82%**	**413**	**18**	**919**	**30.59%**	**21.89**
=6	98.91%	182	2	1166	13.48%	10.74
max	72.52%	979	371	0	72.52%	24.12

TABLE 6. RESULTS OF 7 VOTE MECHANISM (CCA : ONLY TARGET).

Method	ACC	Correct	Wrong	Skipped	Exe Rate	ITR
>=3	68.96%	871	392	87	64.52%	18.76
>=4	79.67%	733	187	430	54.30%	23.20
>=5	**90.12%**	**538**	**59**	**753**	**39.85%**	**23.80**
>=6	93.53%	289	20	1041	21.41%	14.23
7	98.39%	122	2	1226	9.04%	7.06
max	65.33%	882	468	0	65.33%	16.41

TABLE 7. RESULTS OF 7 VOTE MECHANISM (CCA : TARGET + HARMONICS).

Method	ACC	Correct	Wrong	Skipped	Exe Rate	ITR
>=3	69.85%	885	382	83	65.56%	19.73
>=4	81.08%	750	175	425	55.56%	24.88
>=5	**90.91%**	**550**	**55**	**745**	**40.74%**	24.94
>=6	93.38%	296	21	1033	21.93%	14.50
7	99.21%	126	1	1223	9.33%	7.53
max	66.44%	897	453	0	66.15%	17.47

Table 8 lists and compares the four most representative methods. From the results, we can see that using CCA without a voting mechanism produces accuracy of 72.30% and the largest number of correct trials. However, this level of accuracy is not ideal when compared with other proposed SSVEP-based BCI [2]. The poor CCA performance may be caused by the lack of channel number, the design of the visual stimulation interface, and the experiment environment. As mentioned, we adopt only two channels with dry sensors for the convenience of being able to wear the cap. The design of the visual stimulation in our system is different from the traditional design because we have embedded small icons to indicate the options. The experiment is conducted in a general room rather than the shielded room commonly adopted for EEG recording. All these may also be the reasons why the overall accuracy and ITR performance of this system is relatively low when compared with previous SSVEP-BCI studies. From the results of the six-vote method, we can see that accuracy is improved and the number of misclassification trials is significantly suppressed. However, the number of correct trials or the execution rate is dramatically reduced. Since reducing the number of wrong trials is more important, considering the usability of this system, the seven-vote method is adopted, as the number of wrong trials is effectively suppressed in this method. Although the execution rate is still not ideal, the number of wrong trials

is reduced. As explained previously, wrong trials may lead to unpleasant and time-wasting page switch, whereas a low execution rate only slows execution. From all the results shown, we conclude that the seven-vote method is the most suitable method for our system.

TABLE 8. COMPARISON OF THE BEST METHODS.

Method	ACC	Correct	Wrong	Skipped	Exe Rate	ITR
CCA (target + harmonics)	72.30%	**976**	374	0	72.30%	23.85
6 Votes >=4	89.31%	677	81	592	50.15%	**29.21**
6 Votes >=5	95.82%	413	**18**	919	30.59%	21.89
7 Votes (CCA target) >=5	90.12%	538	59	753	39.85%	23.80
7 Votes (CCA target+ harmonics) >=5	**90.91%**	550	**55**	745	40.74%	**24.94**

To furtherly illustrate the performance of the selected algorithm with the adopted flickering frequencies, the confusion matrix is shown in Table 9. The classification accuracy of each frequency is shown in ACC column. Although 24Hz is less accurate compared with other frequencies due to the weaker response for higher flickering frequencies [21], the overall accuracy shows that it is usable and the selection of frequencies is appropriate.

TABLE 9. CONFUSION MATRIX OF 7 VOTES (CCA TARGET + HARMONICS).

	14Hz	16Hz	18Hz	20Hz	24Hz	Skipped	ACC
14Hz	154	0	4	6	0	106	93.9%
16Hz	5	76	0	5	0	184	88.4%
18Hz	5	0	145	1	0	119	96.0%
20Hz	9	2	0	107	0	152	90.7%
24Hz	9	1	1	7	68	184	79.1%
Skipped	0	0	0	0	0	0	N/A
Total	182	79	150	126	68	745	N/A

B. User feedback and feasibility test

User feedback about this assistive system was collected via questionnaire and verbal communication with 15 invited subjects. All subjects agreed that the operating procedure was convenient, the functions provided would meet their needs if they were unable to use their hands, the movement of the robotic arm was safe, and no discomfort was experienced when wearing the wireless dry sensor EEG cap or staring at the flickering screen. Most subjects preferred the seven-vote method to the six-vote method because wrong decisions significantly detracted from their user experience, whereas skipping trials attracted little of their attention. Therefore, although the six-vote method achieved the highest ITR and had comparable accuracy to the seven-vote method, we nevertheless adopted the seven-vote method in our system.

Three of the 15 subjects were invited to test the feasibility of this assistive system after the finalization of voting method based on offline testing results. The participants were asked to make selections following a randomly predetermined list during the online test. An average accuracy of 85% were achieved supporting the feasibility of the system.

IV. CONCLUSION

In this study, we extended our proposed wireless SSVEP-based BCI assistive eating system into a multifunctional assistive system that provides many more functions and services to the user. This system not only provides more services than currently proposed BCI systems; it also offers functions that are more interactive. To make the system more applicable and convenient, we have successfully reduced the time cost caused by wrong decision through the adoption of harmonic components and extended voting mechanisms. The average classification accuracy and ITR achieved is 90.91% and 24.94 respectively. Because this study contributes more to the integration of multiple interactive services and the applicability of the BCI assistive system, there is room for improvement in our investigation of signal characteristics and the development of a classification algorithm. Furthermore, as the main potential users of our system would be the elderly, and age is considered a factor influencing SSVEP-based BCI performance, to furtherly improve our system and work with hospitals to recruit old people or patients with disabilities for validating system usability and feasibility are also important. Our group will therefore focus on these aspects in our future work.

REFERENCES

[1] W. Soogil, S. Younghak, L. Seungchan, and L. Heung-No, "Review of applications for wireless brain-computer interface systems," in G. R. Naik (Ed.), Emerging Theory and Practice in Neuroprosthetics, Hershey, PA: IGI Global, 2014, pp. 128-152.

[2] C. Xiaogang, W. Yijun, G. Shangkai, J. Tzyy-Ping, and G. Xiaorong, "Filter bank canonical correlation analysis for implementing a high-speed SSVEP-based brain–computer interface," Journal of Neural Engineering, vol. 12, no. 4, p. 046008, 2015.

[3] J. M. Dennis, J. K. Dean, A. S. William, and R. W. Jonathan, "Emulation of computer mouse control with a noninvasive brain-computer interface," Journal of Neural Engineering, vol. 5, no. 2, p. 101-110, 2008.

[4] J. R. Wolpaw and D. J. McFarland, "Control of a two-dimensional movement signal by a noninvasive brain-computer interface in humans," Proceedings of the National Academy of Sciences of the United States of America, vol. 101, no. 51, pp. 17849-17854, December 21, 2004.

[5] T. A. Kayagil et al., "A binary method for simple and accurate two-dimensional cursor control from EEG with minimal subject training," Journal of NeuroEngineering & Rehabilitation (JNER), vol. 6, pp. 1-16, 2009.

[6] L. J. Trejo, R. Rosipal, and B. Matthews, "Brain-computer interfaces for 1-D and 2-D cursor control: Designs using volitional control of the EEG spectrum or steady-state visual evoked potentials," IEEE Transactions on Neural Systems and Rehabilitation Engineering, vol. 14, no. 2, pp. 225-229, 2006.

[7] F. Galán et al., "A brain-actuated wheelchair: Asynchronous and non-invasive brain-computer interfaces for continuous control of robots," Clinical Neurophysiology, vol. 119, no. 9, pp. 2159-2169, 2008.

[8] K. Tanaka, K. Matsunaga, and H. O. Wang, "Electroencephalogram-based control of an electric wheelchair," IEEE Transactions on Robotics, vol. 21, no. 4, pp. 762-766, 2005.

[9] H. Cecotti, "A self-paced and calibration-less SSVEP-based brain-computer interface speller," IEEE Transactions on Neural Systems and Rehabilitation Engineering, vol. 18, no. 2, pp. 127-133, 2010.

[10] C. Neuper, G. R. Müller-Putz, R. Scherer, and G. Pfurtscheller, "Motor imagery and EEG-based control of spelling devices and neuroprostheses," in N. Christa and K. Wolfgang (Eds.), Progress in Brain Research, vol. 159, Elsevier, 2006, pp. 393-409.

[11] M. Nakanishi, Y. Wang, Y.-T. Wang, Y. Mitsukura, and T.-P. Jung, "A high-speed brain speller using steady-state visual evoked potentials," International Journal of Neural Systems, vol. 24, no. 6, pp. 1450019-1450019, 2014.

[12] W. Yu-Te, W. Yijun, and J. Tzyy-Ping, "A cell-phone-based brain–computer interface for communication in daily life," Journal of Neural Engineering, vol. 8, no. 2, p. 025018, 2011.

[13] B. Graimann, B. Allison, and G. Pfurtscheller, "Brain-computer interfaces: A gentle introduction," in Brain-Computer Interfaces: Revolutionizing Human-Computer Interaction, in B. Graimann, G. Pfurtscheller, and B. Allison, (Eds.), Berlin, Heidelberg: Springer, 2010, pp. 1-27.

[14] C.-T. Lin et al., "Review of wireless and wearable electroencephalogram systems and brain-computer interfaces: A mini-review," Gerontology, vol. 56, no. 1, pp. 112-119, 2010.

[15] R. Fazel-Rezai, B. Allison, C. Guger, E. Sellers, S. Kleih, and A. Kübler, "P300 brain computer interface: Current challenges and emerging trends," (in English), Frontiers in Neuroengineering, Review vol. 5, no. 14, 2012-July-17 2012.

[16] S.-K. Yeom, S. Fazli, K.-R. Müller, and S.-W. Lee, "An efficient ERP-based brain-computer interface using random set presentation and face familiarity," (in English), PLoS One, vol. 9, no. 11, p. e111157, Nov 2014.

[17] F. Pichiorri et al., "9. Brain network modulation following motor imagery BCI-assisted training after stroke," Clinical Neurophysiology, vol. 126, no. 1, p. e3, 2015.

[18] J. J. M. D. Shih, D. J. P. Krusienski, and J. R. M. D. Wolpaw, "Brain-computer interfaces in medicine," (in English), Mayo Clinic Proceedings, vol. 87, no. 3, pp. 268-79, 2012

[19] W. Ruimin, W. Wu, K. Iramina, and G. Sheng, "The combination of CCA and PSDA detection methods in a SSVEP-BCI system," in Proceedings of the 11th World Congress on Intelligent Control and Automation, 2014, pp. 2424-2427.

[20] C. T. Lin, Y. T. Liu, S. L. Wu, Z. Cao, Y. K. Wang, C. S. Huang, et al., "EEG-Based Brain-Computer Interfaces: A Novel Neurotechnology and Computational Intelligence Method," IEEE Systems, Man, and Cybernetics Magazine, vol. 3, pp. 16-26, 2017.

[21] Y. Wang, R. Wang, X. Gao, and S. Gao, "Brain-computer interface based on the high-frequency steady-state visual evoked potential," in Proceedings of the 2005 First International Conference on Neural Interface and Control, 2005, pp. 37-39.

[22] R. Kus et al., "On the quantification of SSVEP frequency responses in human EEG in realistic BCI conditions," (in English), PLoS One, vol. 8, no. 10, p. 0077536, Oct 2013.

[23] M. Nakanishi, Y. Wang, Y.-T. Wang, Y. Mitsukura, and T.-P. Jung, "Generating visual flickers for eliciting robust steady-state visual evoked potentials at flexible frequencies using monitor refresh rate," (in English), PLoS One, vol. 9, no. 6, p. 0099235, Jun 2014.

[24] R. M.-P. Gernot, S. Reinhold, B. Christian, and P. Gert, "Steady-state visual evoked potential (SSVEP)-based communication: Impact of harmonic frequency components," Journal of Neural Engineering, vol. 2, no. 4, p. 123-130, 2005.

[25] Y. Zhang et al., "Multiway canonical correlation analysis for frequency components recognition in SSVEP-based BCIs," in Proceedings of the 18th International Conference on Neural Information Processing, ICONIP 2011, Part I, 2011, pp. 287-295.

[26] C. Y. Chiu, A. K. Singh, Y. K. Wang, J. T. King, and C. T. Lin, "A wireless steady state visually evoked potential-based BCI eating assistive system," in 2017 International Joint Conference on Neural Networks (IJCNN), 2017, pp. 3003-3007.

[27] A. Petroni, S. S. Cohen, L. Ai, N. Langer, S. Henin, T. Vanderwal, et al., "Age and sex modulate the variability of neural responses to naturalistic videos," bioRxiv, 2017.

CHIN-TENG LIN (S'88–M'91– SM'99–F'05) received the M.S. and Ph.D. degrees in electrical engineering from Purdue University, West Lafayette, IN, USA, in 1989 and 1992, respectively. He is currently the Distinguished Professor of Faculty of Engineering and Information Technology, University of Technology Sydney, University Chair Professor of Electrical and Computer Engineering, NCTU, International Faculty of University of California at San-Diego (UCSD), and Honorary Professorship of University of Nottingham. Dr. Lin was elevated to be an IEEE Fellow for his contributions to biologically inspired information systems in 2005, and was elevated International Fuzzy Systems Association (IFSA) Fellow in 2012. Dr. Lin received the IEEE Fuzzy Systems Pioneer Awards in 2017. He was elected as the Editor-in-chief of IEEE Trans. on Fuzzy Systems in 2011-2016. He also served on the Board of Governors at IEEE Circuits and Systems (CAS) Society in 2005-2008, IEEE Systems, Man, Cybernetics (SMC) Society in 2003-2005, and IEEE Computational Intelligence Society (CIS) in 2008-2010. Dr. Lin is the Distinguished Lecturer of IEEE CIS Society from 2015-2017. He served as the Deputy Editor-in-Chief of IEEE Trans. on Circuits and Systems-II in 2006-2008. He has published more than 280 journal papers (Total Citation: 17,837, H-index: 61, i10-index: 216) in the areas of fuzzy systems, neural networks and cognitive neuroengineering, including approximately 130 IEEE journal papers.

CHING-YU CHIU received the B.S. degree in department of photonics from National Cheng Kung University, Tainan, Taiwan in 2013, and the M.S. degree in Institute of Imaging and Biomedical Photonics from National Chiao Tung University, Hsinchu, Taiwain, in 2016. She is currently working toward the Ph.D. degree at Centre for Artificial Intelligence, Faculty of Engineering and Information Technology, University of Technology Sydney, Australia. Her research interests include brain-computer-Interfaces, signal processing, and machine learning.

AVINASH KUMAR SINGH is currently pursuing the joint Ph.D. degree with the Brain Research Centre, National Chiao Tung University, Hsinchu, Taiwan, and the Computational Intelligence and Brain Computer Interface Centre, University of Technology, Sydney, Australia. His current research interests include improving the performance of the brain_computer interface in the context of traditional, virtual reality, and realworld applications.

JUNG-TAI KING received the B.S. degree in psychology from the National Cheng-Chi University in 1998, the M.S. degree in criminology from the National Chung-Cheng University in 2001, and the Ph.D. degree in neuroscience from National Yang-Ming University, Taiwan in 2010. He is currently an Assistant Research Fellow with the Brain Research Center, National Yang-Ming University. His research interests include psychophysiology, cognitive and social neuroscience, and neuromarketing.

YU-KAI WANG (M'13) received the B.S. degree in mathematics education from National Taichung University of Education, Taichung, Taiwan, in 2006, the M.S. degree in biomedical engineering from National Chiao Tung University (NCTU), Hsinchu Taiwan, in 2009, and the Ph.D. degree in computer science from NCTU, Hsinchu Taiwan, in 2015. He was a Visiting Scholar with the Swartz Center for Computational Neuroscience, University of California at San Diego, La Jolla, CA, USA, from 2013 to 2014. From 2016-2017, he was a postdoctoral researcher with the Centre for Artificial Intelligence in University of Technology Sydney, Australia. He is currently the Distinguished Professor of Faculty of Engineering and Information Technology, University of Technology Sydney. His current research interests include machine learning, computational neuroscience, biomedical signal processing, and the brain–computer interface.